Desalination and Water Treatment
www.deswater.com

doi: 10.5004/dwt.2023.29776

307 (2023) 50–62
September

Reliable treatment approach for levofloxacin and ciprofloxacin removal from aqueous medium: process modelling, kinetic and isotherm studies

Sabah J. Mohammed[a], Mohanad J. M-Ridha[b], Qahtan Adnan Ali[c], Khalid M. Abed[d,e,*], Saeid Ahmadzadeh[f,g,*]

[a]*Department of Environmental Engineering, College of Engineering, University of Baghdad, Iraq, email: eng.sabah1212@gmail.com*
[b]*Department of Environmental Engineering, College of Engineering, University of Baghdad, Iraq, email: muhannadenviro@coeng.uobaghdad.edu.iq*
[c]*Department of Environmental and Pollution Techniques Engineering, Technical Engineering College/Kirkuk, Northern Technical University, 36001 Kirkuk, Iraq, email: dr.qahtanali@ntu.edu.iq*
[d]*Department of Chemical Engineering, College of Engineering, University of Baghdad, Baghdad, Iraq, email: khalid.chemical82@gmail.com (ORCID iD: 0000-0003-4791-219X)*
[e]*Department of Chemical Engineering, Faculty of Engineering, Universiti Malaya, 50603 Kuala Lumpur, Malaysia*
[f]*Pharmaceutics Research Center, Institute of Neuropharmacology, Kerman University of Medical Sciences, Kerman, Iran, Tel.: +98 3431325241; Fax: +98 3431325215; email: chem_ahmadzadeh@yahoo.com (ORCID iD: 0000-0001-8574-9448)*
[g]*Pharmaceutical Sciences and Cosmetic Products Research Center, Kerman University of Medical Sciences, Kerman, Iran, email: saeid.ahmadzadeh@kmu.ac.ir*

Received 2 May 2023; Accepted 12 July 2023

ABSTRACT

Current work aimed to optimize the electrocoagulation (EC) process for the efficient and economic removal of ciprofloxacin (CIP) and levofloxacin (LVX) from aqueous solution via response surface methodology. Four main parameters were selected for the optimisation process, including the initial pH of the solution, initial concentration of antibiotics, operation time, and current density. Subsequently, kinetic and isotherm modelling was performed to characterise the performance behaviour of the EC process at optimum conditions. Based on the results, the EC process achieved a removal efficiency of 92% and 84% for CIP and LVX, respectively, under optimum experimental conditions. The experimental results were consistent with the Langmuir isotherm model for the adsorption of both antibiotics on the iron hydroxide ($Fe(OH)_3$) flocs based on the predicted maximum adsorption capacity of 142 and 185 mg/g, respectively. In addition, the experimental results best fitted the second-order kinetic model with a coefficient of determination (R^2) value of 0.986 and 0.992 for CIP and LVX, respectively, implying the chemisorption mechanism controlling the adsorption process. The regression analysis also showed that the experimental results best fitted with the second-order polynomial model with a predicted correlation coefficient (Pred. R^2), adjusted correlation coefficient (Adj. R^2), and R^2 of 0.834, 0.941, and 0.967 for CIP; 0.723, 0.908, and 0.952 for LVX, respectively. In short, a comprehensive economic evaluation was performed and the total operational cost over a single run under optimized EC conditions was estimated at \$0.490 US/m^3. Under optimized EC conditions, the electrical energy consumption and electrode consumption were 3 kWh/m^3 and 0.167 kg/m^3, respectively, during a single run.

Keywords: Electrocoagulation; Central composite design; Ciprofloxacin; Levofloxacin; Total operational cost; Wastewater treatment

* Corresponding authors.

1. Introduction

Over the past several decades, the increased consumption of pharmaceutical products and veterinary medicine has led to the overwhelming discharge of effluents into water bodies containing harmful wastes and by-products from these compounds, particularly antibiotics and their metabolites. The growing concern over such practices has thus been considered a major environmental and public health issue [1,2]. Several classes of antibiotics, such as ciprofloxacin and levofloxacin, are among the most frequently detected pharmaceutical compounds in numerous aquatic environments, including surface water, groundwater, and in a few cases drinking water. Pharmaceutical compounds, especially antibiotics and growth hormones, can cause detrimental environmental effects as they affect the quality of soil, surface water, and groundwater [3,4]. Moreover, the presence of pharmaceutical residues in sewage treatment plant (STP) effluents presents a huge drawback for biological treatment technologies given the severe toxic properties of antibiotics against microbial populations that are essential in wastewater treatment processes [5,6]. The harmful effect of antibiotics on biological wastewater approaches would allow antibiotics to seep through STP systems and infiltrate surface water, drinking water, groundwater, and soil, leading to the emergence of antibiotic-resistant microbial pathogens [7,8].

Fluoroquinolones (FQs) are one of the largest antibiotic groups that exhibit high chemical stability and are unable to be completely digested in the human body. Humans and animals eliminate undigested FQs through urinary excretion, where they flow into conventional wastewater treatment plants (CWWTPs) [9,10]. Since FQs pose harmful toxic effects to microbial activities, they commonly undergo limited degradation in biological treatment systems and are discharged back into the environment. In the long run, FQs may adversely affect the health of humans and other organisms even at trace concentrations. Their ubiquitous presence in ecosystems is therefore identified as hazardous emerging pollutants. In this regard, it is essentially crucial to design a suitable and cost-effective treatment technique to remove these adverse compounds [11,12].

Ciprofloxacin (CIP) is a synthetic second-generation FQs that has been extensively applied to treat various infectious bacterial diseases in humans and animals. Apart from the partial metabolic breakdown in humans and improper disposal of unused or obsolete CIPs, the lack of appropriate facilities in conventional WWTPs to treat discharge containing CIP residues from drug manufacturers and hospitals has resulted in the rising contamination of CIP in surface water in the recent decade [13]. It was proclaimed that the daily consumption of drinking water containing traces of CIP may cause nausea, nervousness, headaches, vomiting, tremors, and diarrhoea. Conversely, a higher concentration of CIP in contaminated drinking water may lead to severe adverse effects, such as leucopenia, eosinophilia, acute renal failure, thrombocytopenia, and elevated expression of liver enzymes. According to a recent statistic published by the health community, the allowed concentration of CIP in surface and underground water should be less than 1 μg/L. Nevertheless, the amount of CIP in wastewater from drug manufacturers and hospitals was found to exceed the safety limit by up to 50 mg/L and 150 μg/L, respectively, which is severely detrimental to human health [14].

Levofloxacin (LVX) is a third-generation antibiotic belonging to FQs and is an active optical isomer of ofloxacin with susceptible anti-bacterial activities against a wide spectrum of microbial species and *Streptococcus* than the previous groups. LVX has been broadly utilised to treat multiple infectious diseases, including pneumonia and abdominal infections. Similar to CIP, LVX exhibits exceptional resilience to degradation and typically seeps through conventional STP systems. In addition, the absence of specific treatment processes that target LVX contributes to its widespread discharge in the aquatic environment. LVX has been observed in various water sources at dissimilar concentration levels, which may reach up to 87.4 ng/L [4,15]. The consistent discharge of LVX in water bodies would consequently lead to the increased bioaccumulation of LVX in the aquatic environment and therefore trigger severe toxicity to marine life and humans [16]. Releasing this antibiotics into the environment increases the levels of antibiotic resistant bacteria, which makes the treatment process more challenging. Conventional wastewater treatment systems can be ineffective in removing prescription antibiotics. As a result, there is a rising need to develop more effective solutions to treat these pollutants [17,18].

Recent literature studies have shown a rising interest in the development of efficient and economical methods for the removal of antibiotic contaminants from wastewater and drinking water supply before being safely released into the environment. Several promising approaches to treat antibiotic-contaminated wastewater have been proposed, such as adsorption, and advanced oxidation process. Remarkably, the electrocoagulation (EC) approach has received the most attention over its extensive practical application for the treatment of different wastewaters with satisfactory outcomes [19,20]. The primary reaction in a typical EC process is the simultaneous metal electrode dissolution in the anodic part and the generation of hydroxyl ions in the cathodic part. Ultimately, the dissolved charged metal hydroxides eliminate the available soluble inorganic pollutants. In view of this, EC has been employed as an efficient and economical method to treat numerous wastewater sources, such as paper-making and laundry processes, reactive dyes, heavy metals and antibiotics. EC can also be used to remove pharmaceutical residues through adsorption and charge neutralization [21,22].

Meanwhile, the central composite design (CCD) is a compelling analytical tool to improve the efficiency of contaminant removal by optimising the operating conditions based on the response surface methodology (RSM). RSM comprise a set of statistical and mathematical methods that optimize the process factors and formulate quadratic models to provide a valuable statistical relationship between the studied variables. The main goal of RSM is to evaluate the optimum operational conditions of a system or to estimate a region that satisfies the operating conditions [23,24]. Recent studies have also used RSM to optimize the treatment of azo dye, heavy metals, industrial effluent, and pharmaceutical wastewater [25,26].

Realising the need to seek an alternative method to treat antibiotics-containing wastewater, this study was performed

to optimize the experimental conditions of the EC process with stainless steel electrodes for the removal of CIP and LVX from an aqueous solution via the CCD-based RSM approach. The main operating parameters that influence the removal efficiency of the EC process were assessed, including the initial antibiotic concentration, pH value, current density, and operating time. Following the optimization process, kinetic and isotherm modelling was carried out to characterise the removal performance behaviour under optimized EC conditions. Finally, a thorough economic evaluation was conducted to estimate the total operating cost of the proposed EC process. Overall, the EC process employed in this study would offer an effective and economical technique for antibiotic removal from aqueous solutions.

2. Materials and methods

2.1. Chemicals

Ciprofloxacin ($C_{17}H_{18}FN_3O_3{\cdot}HCl{\cdot}H_2O$; purity ≥ 98%; molecular weight, 385.6 g/mol; water solubility, 36 mg/mL at 25°C; λ_{max} = 272 nm) was acquired from Tabuk Pharmaceuticals Manufacturing Company, Kingdom of Saudi Arabia, while levofloxacin ($C_{18}H_{20}FN_3O_4{\cdot}½H_2O$; purity ≥ 98.0%; molecular weight, 370.38 g/mol; water solubility, 272 mg/mL at 25°C; λ_{max} = 293 nm) was purchased from Julphar Gulf Pharmaceutical Industries, United Arab Emirates.

Sodium hydroxide (NaOH) and hydrochloric acid (HCl) were obtained from Merck and used to adjust the pH buffers. Meanwhile, sodium chloride (NaCl) (purity ≥ 99.9%; Merck) was used to adjust the initial conductivity of the solution. The metal electrodes were composed of highly purified stainless steel (SS 304, India). All chemical reagents that were used in this work were of analytical reagent grade with the highest available purity. Distilled water was used to prepare all analytical-grade chemical solutions.

2.2. Experimental setup and analytical methods

A simple EC reactor was configured, which consists of a 1 L beaker as the electrolytic cell and a pair of stainless-steel electrode plates (anode and cathode) with a diameter and thickness of 8.5 cm and 2 mm, respectively, and placed horizontally in the reactor. The electrodes were set apart at 1.5 cm and connected to an external power supply (0–30 ± 0.1 V, 0–5 ± 0.1 A) (DC model: PS.305D). As a result of the oxidation reaction, carcass electrodes dissolve in the watercourse and should be frequently restored. Hence, stainless steel electrodes were utilised in the reactor due to their ability to extend the longevity of the treatment system and minimise the need for maintenance. Prior to each experiment, 0.2 M HCl was used to wash the electrodes for 2 min, followed by rinsing with distilled water and drying.

The EC experiments were performed using 1,000 mL of samples. The pH of the sample solution was measured using a laboratory pH meter (ISOLAB, Germany) and adjusted using 0.01 N NaOH or HCl, while the conductivity of the sample solution was increased using 500 mg/L of NaCl. The sample was then stirred using a magnetic stirrer (ISOLAB, Germany) at a fixed stirring speed of 120 rpm during the operating time. All experiments were performed in batch mode. At the end of the operating time, samples were collected from the EC reactor and the suspensions were left to stabilise for 30 min. Then, a membrane filter with a pore size of 0.45 μm (Whatman, Germany) was used to filter the samples before being analysed using a UV-Visible Spectrophotometer (UV-1800 Shimadzu, Japan). The method for the removal of pollutants resembles the conventional adsorption technique except that the EC process generates coagulants or flocs. Generally, the electrochemically generated flocs adsorb pollutants onto their surface following two successive processes: (i) the generation of iron hydroxide ($Fe(OH)_3$) flocs through an electrochemical process and (ii) the adsorption of pollutants on the surface of the flocs via the physico-chemical process [27]. Besides, the electrode consumption (ELC) was evaluated according to Faraday's law and the amount of flocs generated was determined through stoichiometric calculation. The developed iron hydroxide flocs trap the available pollutants in the solution via adsorption. In addition, the amount of ELC in the EC process was estimated according to Faraday's law [Eq. (1)] [28,29].

$$\mathrm{ELC} = \frac{ItM}{zF} \tag{1}$$

where ELC is the amount of electrode consumed (g), I denotes the applied current (A), t is the operation time (sec), M refers to the molecular weight of iron (g/mol), z represents the number of electrons, and F refers to Faraday constant (96,485°C/mol). Furthermore, the electrical energy consumption (EEC)of the EC process (kWh/m^3) was measured according to Eq. (2) [30,31]:

$$\mathrm{EEC} = \frac{UIt}{V} \tag{2}$$

where U refers to the applied voltage (V), I is the applied current (A), t denotes the operation time (h), and V is the volume of the sample (L).

2.3. Economic evaluation

Cost analysis is a vital element in the development of cost-effective wastewater treatment technology. The cost of the EC process includes the cost of electrode dissolution, the cost of energy consumption, and the cost of additional chemicals, such as NaOH and HCl to modify the pH values of the solution or NaCl to boost the conductivity of the solution. The working cost was estimated in the EC process based on Eq. (3) [32]:

$$\text{Operating cost} = a\,\mathrm{ELC} + b\,\mathrm{EEC} + c\,\mathrm{CC} \tag{3}$$

where a represents the price of the electrode material ($US/kg), ELC is the quantity of electrode consumed (kg/m^3), b denotes the price of electrical energy ($US/kWh), EEC is the amount of electrical energy consumed (kWh/m^3), c refers to the price of the additional chemicals used ($US/kg), and CC describes the amount of chemical consumption (kg/m^3).

2.4. Process variables and experimental design for the CCD approach

In the present study, the CCD technique was applied to assess the effect of several parameters on the contaminant

removal efficiency based on the optimization of the operating variables of the EC method using RSM. The optimization process involves the three main steps: (i) statistical design of the experiment, (ii) applying a mathematical model to estimate the coefficient values, and (iii) predicting the response and verifying the suitability of the applied model.

Four parameters that affect the removal of the antibiotic were selected (*A*: initial concentration of antibiotics, *B*: pH value, *C*: current density, *D*: operation time) and each parameter was optimized under specific ranges to achieve optimal conditions for the EC process. Table 1 shows the selected parameters and their operating ranges.

The design of the experimental parameters and statistical analysis of the EC process was conducted using the Design-Expert software version 12.0.2.0. In addition, the verification of the accuracy value of the model's adequacy was determined using analysis of variance (ANOVA).

Furthermore, experimental data from the CCD for the antibiotic removal efficiency was examined and fitted to an overall function to indicate the reaction between the independent and dependent operating variables through the second-order polynomial equation, as follows [33]:

$$Y = \beta_o + \sum_{i=1}^{n} \beta_i X_i + \sum_{i=1}^{n} \beta_{ii} X_i^2 + \sum_{i=1}^{n-1} \sum_{j=i+1}^{n} \beta_{ij} X_i X_j \quad (4)$$

where Y denotes the expected response to remove the contaminant, β_0 refers to the intercept parameter, β_i is the linear coefficients, β_{ii} describes the quadratic coefficients, β_{ij} implies the interaction coefficients, and X_i and X_j represent the coded values of the independent factors.

2.5. Adsorption kinetics study

A thorough insight into the reaction pathway and the corresponding sorption mechanism, which relies on the physico-chemical characteristics of the adsorbent as well as the mass-transfer process, can be explored by conducting the adsorption kinetics study. The adsorption kinetic studies of the CIP and LVX removal at different concentrations were performed under optimized EC conditions. Following the sample collection at 8, 12, 16, 20, 30, and 48 min, the kinetic parameters were computed, and the removal mechanism was described using three models, namely, first-order, second-order, and pseudo-first-order.

2.6. Isotherm modelling

The development of the isotherm modelling with an appropriate correlation for the equilibrium curve offers essential input on the adsorption mechanism. Hence, the adsorption of antibiotics on the surface of the generated iron hydroxide flocs was assessed via two general adsorption isotherms, which consist of the Freundlich and Langmuir models. The isotherm modelling was performed under optimized EC conditions with varying CIP and LVX concentrations of 6, 12, 24, 36, and 48 mg/L.

3. Results and discussion

3.1. Statistical design and analysis

The CCD-based RSM was used to optimize the CIP and LVX removal efficiency from aqueous solutions. Four experimental parameters were selected, namely the initial antibiotics concentration, the pH value of the solution, current density, and operating time. The values of the operating variables were subjected to the Design of Expert (DOE) to determine the best removal efficiency. Table 2 describes the summary of the experimental parameters together with the findings from 30 trials according to the RSM.

3.2. ANOVA results

The data were built-in into the quadratic model to determine the mathematical relationship between the applied factors and the observed response.

3.2.1. Final equation in terms of the coded factors

The coded equation is instrumental to compare the factor coefficients and determine the relative impact of the factors. The final equation in terms of the coded factors was applied to predict the response of each factor for the given levels. By default, low-level factors are coded as –1 while high-level factors are coded as +1. The obtained equations from the RSM model are expressed as the following:

$$\begin{aligned}\text{Removal of CIP}(\%) = {} & +73.29 - 1.98A - 7.35B + 3.32C \\ & + 6.13D + 1.09AB + 0.8350AC \\ & + 0.6925AD + 0.9625BC \\ & - 0.8150BD + 0.7487CD \\ & - 1.97A^2 + 0.4015B^2 + 0.9397C^2 \end{aligned} \quad (5)$$

$$\begin{aligned}\text{Removal of LVX}(\%) = {} & 67.01 - 08536A - 9.60B + 1.17C \\ & + 3.88D - 1.74AB - 2.47AC \\ & - 0.1119AD + 0.9256BC \\ & - 0.8044BD + 1.08CD - 2.98A^2 \\ & + 2.00B^2 + 0.3020C^2 - 0.9792D^2 \end{aligned} \quad (6)$$

Table 1
Actual and coded values of the numeric factors for each parameter

Coded variables (X_i)	Factors	Experimental field				
		–α	–1 level	0	+1 level	+α
X_1	*A*: Initial concentration (mg/L)	5.00	24.87	52.50	80.13	100.00
X_2	*B*: pH of solution	3.00	3.84	5.00	6.16	7.00
X_3	*C*: Current density (mA/cm²)	5.00	8.14	12.50	16.86	20.00
X_4	*D*: Time of electrolysis (min)	5.00	16.50	32.50	48.50	60.00

Table 2
Experimental conditions of the four selected parameters in the CCD matrix and the respective CIP and LVX removal with predicted response values vs. actual response values based on the proposed RSM model

Run order	Actual values				CIP		LVX	
	Factor 1 *A*: C_o (mg/L)	Factor 2 *B*: pH	Factor 3 *C*: CD (mA/cm^2)	Factor 4 *D*: t (min)	*R* (%) (Actual value)	*R* (%) (Predicted value)	*R* (%) (Actual value)	*R* (%) (Predicted value)
1	52.50	5.00	12.50	5.00	61.00	62.75	53.00	57.44
2	80.13	6.16	16.86	16.50	63.00	62.78	51.00	48.73
3	24.87	6.16	8.14	16.50	56.00	58.89	50.00	51.67
4	24.87	3.84	8.14	48.50	85.96	87.07	71.85	75.07
5	52.50	5.00	12.50	32.50	73.50	73.29	66.00	67.01
6	24.87	6.16	8.14	48.50	69.13	66.65	53.75	55.89
7	52.50	5.00	20.00	32.50	78.18	81.77	69.6	69.91
8	80.13	3.84	8.14	48.50	81.00	80.64	80.00	81.57
9	80.13	6.16	8.14	48.50	63.00	64.57	57.37	55.42
10	80.13	3.84	8.14	16.50	68.00	66.86	73.82	74.58
11	52.50	5.00	12.50	60.00	82.57	83.83	75.80	70.80
12	80.13	6.16	8.14	16.50	55.00	54.05	52.85	51.65
13	24.87	3.84	16.86	48.50	93.73	91.61	82.00	82.67
14	52.50	5.00	12.50	32.50	73.86	73.29	67.00	67.01
15	52.50	5.00	12.50	32.50	74.00	73.29	67.49	67.01
16	24.87	6.16	16.86	48.50	73.00	75.03	67.00	67.19
17	24.87	3.84	16.86	16.50	78.28	77.60	68.00	70.90
18	80.13	3.84	16.86	48.50	90.52	88.52	80.00	79.28
19	52.50	5.00	5.00	32.50	71.00	70.37	66.77	65.90
20	52.50	5.00	12.50	32.50	72.79	73.29	67.50	67.01
21	5.00	5.00	12.50	32.50	70.00	70.89	62.00	59.69
22	52.50	5.00	12.50	32.50	75.35	73.29	66.50	67.01
23	80.13	6.16	16.86	48.50	78.00	76.30	53.00	56.83
24	52.50	3.00	12.50	32.50	84.00	87.10	90.00	89.41
25	24.87	3.84	8.14	16.50	77.43	76.05	72.00	67.63
26	52.50	5.00	12.50	32.50	73.40	73.29	67.00	67.01
27	52.50	7.00	12.50	32.50	62.00	61.85	56.38	56.40
28	80.13	3.84	16.86	16.50	72.33	71.74	70.64	67.96
29	24.87	6.16	16.86	16.50	67.00	64.28	60.75	58.64
30	100.00	5.00	12.50	32.50	62.00	64.07	55.00	56.75

3.2.2. Final equation in terms of the actual factors

The final equation in terms of the actual factors was utilised to predict the response of each factor for the given levels. In contrast to the final equation in terms of the coded factors, the equation should not be applied to measure the relative impact of each factor since the coefficients were defined to accommodate the original unit of each factor and the intercept is not at the centre of the design space. The obtained equations of the RSM model are expressed as follows:

$$\begin{aligned}\text{Removal of CIP}(\%) = {} & 119.881 - 0.108\text{Co} - 12.003\text{pH} \\ & - 2.134CD + 0.386t + 0.034\text{Co}\times\text{pH} \\ & + 0.007\text{Co}\times D + 0.002\text{Co}\times t \\ & + 0.190\text{pH}\times CD - 0.044\text{pH}\times t \\ & + 0.011CD\times t - 0.003\text{Co}^2 \\ & + 0.297\text{pH}^2 + 0.049CD^2 \end{aligned} \quad (7)$$

$$\begin{aligned}\text{Removal of LVX}(\%) = {} & 105.765 + 0.914\text{Co} - 21.024\text{pH} \\ & - 0.468CD + 0.527t - 0.054\text{Co}\times\text{pH} \\ & - 0.021\text{Co}\times CD - 0.0003\text{Co}\times t \\ & + 0.182\text{pH}\times CD - 0.043\text{pH}\times t \\ & + 0.015CD\times t - 0.004\text{Co}^2 \\ & + 1.474\text{pH}^2 + 0.016CD^2 - 0.004t^2 \end{aligned} \quad (8)$$

3.2.3. ANOVA evaluation

The suitability of the developed model was verified and summarised based on the experimental results, as presented in Table 3.

The *F*-values of 36.38 and 21.32 for CIP and LVX, respectively, implied the significance of the model. In other words, there is only a 0.01% probability that the result could occur due to noise. The *p*-values of less than 0.0500 for CIP (*A*, *B*,

Table 3
ANOVA results of the response surface of the quadratic model

Response	Source	Sum of squares	Degree freedom	Mean square	*F*-value	*p*-value	Significance
Removal of CIP (%)	Model	2,491.60	13	191.66	36.38	<0.0001	Significant
	Residual	84.29	16	5.27	–	–	–
	Lack of fit	80.57	11	7.32	9.86	0.0102	Significant
	Pure error	3.71	5	0.7429	–	–	–
Removal of LVX (%)	Model	2,828.47	14	202.03	21.32	<0.0001	Significant
	Residual	142.15	15	9.48	–	–	–
	Lack of fit	140.45	10	14.05	41.39	0.0004	Significant
	Pure error	1.70	5	0.3393	–	–	–

C, *D*, and A^2) indicate that the model terms were significant. Similarly, the *p*-values of less than 0.0500 for LVX (*B*, *D*, *AB*, *AC*, A^2, and B^2) indicate the significance of the model terms. In contrast, *p*-values greater than 0.1000 indicate insignificant model terms [33,34]. A model reduction could be applied to enhance the model in the case of excessive insignificant model terms (excluding those required to support hierarchy). Furthermore, the Lack-of-Fit of the *F*-value of 9.86 and 41.39 for CIP and LVX, respectively, implied the significance of the Lack-of-Fit. In other words, there is only a 1.02% and 0.04% probability for CIP and LVX that the result could occur due to noise. For the model to fit, a significant Lack-of-Fit should be avoided [34].

3.2.4. Fit statistics

According to the regression analysis, the experimental data were better fitted to the second-order polynomial model with a pred. R^2, Adj. R^2, and R^2 of 0.834, 0.941, and 0.967 for CIP and 0.723, 0.908, and 0.952 for LVX, respectively. The difference between Pred. R^2 and Adj. R^2 was less than 0.2 for both CIP and LVX, demonstrating that the predicted models and experimental results were in good agreement. Additionally, the AP value denotes the signal-to-noise ratio with a favourable ratio of greater than 4. Based on the results, the CIP and LVX recorded an AP of 23.954 and 18.691, respectively, indicating an adequate signal. Therefore, the model agrees with the results from past studies [14,35,36] and was employed to navigate the design space.

3.3. Predicted vs. actual model

A significant part of the analytical process is the adequacy checks of the suggested models. Fig. 1a and b illustrate the comparison between the experimental response values and expected response values from the developed model. It was noted that the predicted model matched the actual values and that the data points were located near the diagonal line for both CIP and LVX. In addition, the ANOVA of the regression model for both quadratic equations was significant (*p*-value < 0.0001). The analysis also revealed that the second-order polynomial equations adequately predict the efficiency of CIP and LVX removal in the EC process. The adequacy of the models was further verified using the R^2. As calculated, the R^2 values of the quadratic equations for CIP and LVX were 0.967 and 0.952, respectively, which signifies that the models fitted well with the data.

3.4. Normal probability

The data were analysed to verify the normality of the residuals, which indicates the extent to which the developed model satisfies the ANOVA assumptions, while the internally studentised residuals measure the standard deviation that distinguishes the predicted and actual values. Besides, a normal probability plot implies that the residual points form a straight line and follow a normal distribution. Nevertheless, scattered data are also expected even with normalised data. Fig. 1c and d show the studentised residuals and the normal probability plots for the removal of CIP and LVX, respectively. Based on the figures, the data were considered normally distributed.

3.5. Box–Cox transformation for the estimation of the best λ-values

In this study, the Box–Cox transformation technique was applied to enhance the statistical analysis. The technique provides a useful guideline to select the appropriate power transformation. The lowest point on the Box–Cox plot denotes the λ-value with the least residual sum of squares (residual SS). Apart from the minimum λ-values (green line), the plot also shows the λ-values in the 95% confidence interval (CI) range (red lines). Conversely, the best λ-value of the power transformation (blue line) is recommended in the absence of a standard transformation within the CI. Although this technique facilitates the transformation of the dependent or independent variables, the computation and interpretation process was preferably simplified by transforming the dependent variables.

Due to the reduced residuals, the goal was to significantly enhance the capability of the models. Thus, the range of the λ-values from −3 and +3 was individually tested for each dependent variable to determine the most favourable transformation. Subsequently, the corresponding residuals in the natural logarithm were plotted against the λ-values for each response, notably for the removal of CIP and LVX. Fig. 1e and f present the required λ-values that were determined by examining all residuals, which correspond to the minimum residuals. Finally, the λ-values were applied to

transform the models. Based on the results, the λ-values for the removal of CIP and LVX were both 1.00. As depicted in Fig. 1e and f, the standard model transformation for the removal of CIP and LVX with all variables and responses was almost identical to the best λ-value within the CI.

3.6. Factors affecting the EC process

The analysis of the main parameters is primarily essential in each optimization study since their adjustment directly impacts the economic costs, particularly the amount of power consumption in the overall process. In this study, the influence of four parameters, including the initial antibiotic concentration, the pH value, current density, and operation time, on the efficiency of removing CIP and LVX antibiotics from an aqueous solution using the EC process were assessed.

3.6.1. Effect of initial concentration of antibiotics

The results revealed that the increased initial concentration and pH value reduced the efficiency of removing CIP and LVX antibiotics. As presented in Fig. 2a and b, the removal efficiency increased from 65% to 80% and 55% to 75% for CIP and LVX, respectively, by decreasing the initial concentration from 80.1 to 52.5 mg/L at the centre point of the significant operational parameters, including the current density at 12.5 of mA/cm^2 and operation time of 32.5 min. This could be due to the insufficient generation of iron hydroxide flocs to adsorb the higher initial concentrations of CIP and LVX.

The initial concentration induces a vital driving force to suppress the mass transfer resistance of the solutes between the solid and aqueous phases. Based on the findings, the removal efficiency decreased with the increased initial concentration of CIP and LVX. Based on the Faraday's law, the generation of iron hydroxide flocs at a constant current density within a certain period remains constant at various concentrations of CIP and LVX. Therefore, at higher CIP and LVX concentrations, the generation of iron hydroxide flocs becomes a limiting factor to remove the excess CIP and LVX. Consequently, the removal efficiency was reduced by a certain percentage due to the reduced conductivity between the limited generation of iron hydroxide flocs and CIP or LVX. These results agreed with the results obtained by Yoosefian et al. [36].

3.6.2. Effect of initial pH values

One of the most significant factors affecting the electrochemical processes is the pH value, especially in the EC process, as they affect the conductivity of the solution, electrode performance, and hydroxide speciation. Numerous

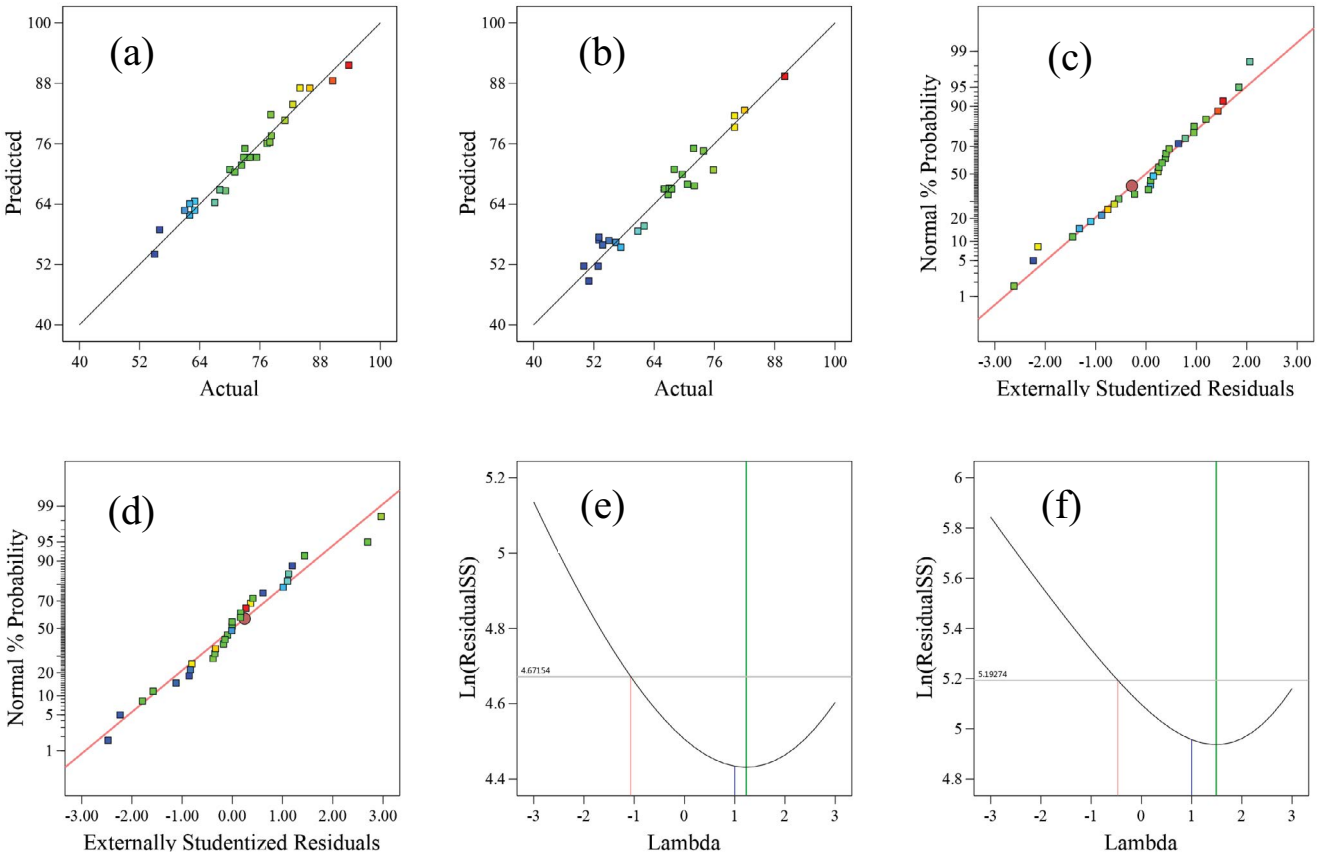

Fig. 1. Predicted model vs. actual model for (a) CIP and (b) LVX. The relationship between the external studentised residuals and normal probability for the removal of (c) CIP and (d) LVX. Box–Cox plot for the power transformation for the removal of (e) CIP and (f) LVX.

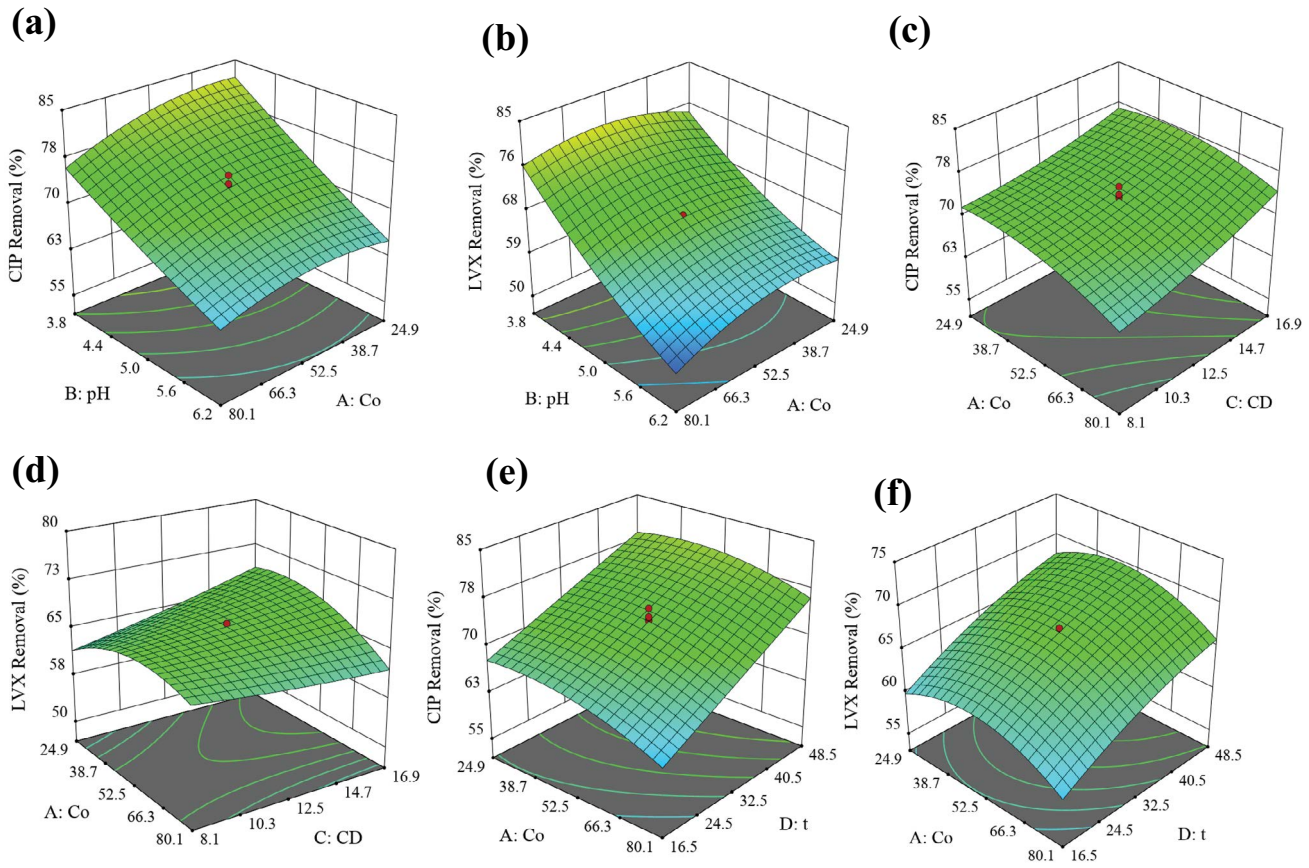

Fig. 2. Effect of the initial concentration and initial pH on the removal efficiency of (a) CIP and (b) LVX. Effect of initial concentration and current density on the removal efficiency of (c) CIP and (d) LVX. Effect of initial concentration and operation time on the removal efficiency of (e) CIP and (f) LVX.

iron hydroxide species are generated in the solution at varying pH values. For instance, $[Fe(OH)_2]^+$ and $Fe(OH)_3$ are the leading type of hydrolysis reactions. Specifically, the electrically generated Fe^{3+} at the anode can be transferred via the hydrolysis process to create a chain of activating ions that destabilise contaminant molecules that exist in the wastewater [21,37]. The destabilised molecules then coagulate to form flocs. To examine the effect of pH on the EC process, both CIP and LVX solutions were adjusted to the desired pH using NaOH or HCl solution.

Following the EC process, the removal percentages of the two antibiotics from aqueous solutions at varying initial pH values were analysed, as illustrated in Fig. 2a and b. When the pH value was reduced from 6.2 to 3.8, the removal efficiency for CIP and LVX increased from 65% to 80% and 55% to 75%, respectively. The phenomenon was associated with the chemical properties of CIP at pH lower than 5.5, which existed almost 99% in the form of CIP^+ (cationic) due to the protonation of the amine group in the piperazine moiety. Interestingly, the generation of $Fe(OH)^{2+}$, $Fe(OH)_2^+$, and $Fe_2(OH)_2^{4+}$ is advantageous for the precipitation of antibiotics. According to the reaction, the scavenging activity of $^{\bullet}OH$ by H^+ increased significantly at extremely low pH ranges, where the protons in the solution were reduced to H_2 at the cathode. Note that the production of hydroxyl and perhydroxyl radicals may have been suppressed by H^+. In contrast, over 95% of CIP molecules exist as CIP^- (anionic) at a pH higher than 7.7 because of the loss of protons from the carboxylic group. Meanwhile, CIP exists as CIP^0 (zwitterion) at a specific pH range 5.5–7.7 due to the balanced charge between the two groups [16,30]. LVX molecules also exist in three forms, primarily as cationic (H_2LVX^+, protonated piper-azinyl group) at pH below 5.0, anionic (LVX^-, deprotonated carboxyl group) at pH above 8.5, and zwitterion ($HLVX^0$, neutral) at a pH range of 5.0–8 [38]. These results agreed with results obtained by Barışçı and Turkay [23].

3.6.3. Effect of current density

Current density is also among the most crucial parameters in electrochemical processes, which controls the reaction rate within the EC reactor. The amount of current density determines the coagulant production rate as well as control the rate and size of the bubble production, which influence the development of the flocs. The strong impact of current density was observed on the kinetics of removal and shortening treatment time of the EC process. A high current density induces a greater generation of iron dissolution in the anode, which provides more precipitate for the removal of pollutants. Moreover, the increased current density enhanced the rate of bubble generation, eventually facilitating a high pollutant removal via H_2 flotation [39,40].

In this study, the EC process was performed at various current densities to evaluate the impact of current density on the efficiency of removing CIP and LVX antibiotics. The results revealed that the increased current density led to an improved removal efficiency of both antibiotics. As observed in Fig. 2c and d, the removal efficiency increased from 68% to 76% and 62% to 68% for CIP and LVX, respectively, when the current density increased from 8.1 to 16.9 mA/cm^2 at the centre point of the significant operational parameters at an initial pH of 5 and operation time of 32.5 min. An increased current density corresponds to the increased ion generation at the anode and cathode, thus, enhancing the removal efficiency. These results agreed with the results obtained by Mohammed et al. [16].

3.6.4. Effect of operation time

The operation time, which refers to the electrolysis time (t), impacts the removal efficiency in the electrochemical process as it controls the rate of production of Fe^{2+} or Fe^{3+} from the iron electrodes. In fact, the removal efficiency directly relies on the concentration of hydroxyl and metal ions that are generated on the electrodes. In short, a greater generation of metal ions provides a sufficient amount of hydroxyl ions to react with the contaminants, hence, increasing the removal efficiency. In this regard, the operation time is a crucial parameter that controls the formation of a sufficient amount of metal ions from the electrodes. Although various studies have reported that the pollutants removal efficiency is enhanced with increased operation time, the operation time becomes the limiting factor and the removal efficiency becomes constant beyond the optimum operation time. Moreover, the removal of any contaminants exhibits specific optimal and ideal reaction times that determine the economic boundaries of the EC process [39,41].

In this study, the operation time was adjusted at a range from 5 to 60 min to assess the impact of operating time on the efficiency of CIP and LVX removal. As illustrated in Fig. 2e and f, the increased operation time from 16.5 to 48.5 min enhanced the efficiency of removing CIP and LVX antibiotics from 65% to 79% and 60% to 68%, respectively, at the centre point of the significant operational parameters at a current density of 12.5 mA/cm^2 and initial pH of 5. The result was assumed to be related to the formation of iron hydroxides from the anode dissolution. At a fixed current density, the generation of iron hydroxide flocs increased with a longer operation time, resulting in improved removal efficiency.

3.6.5. Optimal conditions

The optimal conditions of the four main parameters were applied in the EC process for enhanced efficiency of CIP and LVX removal from the aqueous solution. The results were improved using the regression equation of RSM with CCD. Fig. 3a and b show the maximum removal efficiency of CIP and LVX under optimized EC conditions based on the DOE software analysis.

3.7. Kinetic modelling

The kinetic parameters of the developed models are summarised in Table 4. The adsorption of CIP and LVX on the surface of the $Fe(OH)_3$ and $[Fe(OH)_2]^+$, which act as the main species from the Fe^{3+} hydrolysis, showed the efficient EC process for the efficiency of removing CIP and LVX antibiotics at an equilibrium time of 48 min. Given that the second-order kinetics model best fitted the experimental data with an R^2 of 0.986 for CIP and 0.992 for LVX, it was deduced that the adsorption of both antibiotics on the surface of the formed absorbents occurred via the sweep flocculation mechanism. The results also indicate that the removal of the CIP and LVX was regulated through the chemisorption mechanism. According to past literature related to the EC process on wastewater treatment, the removal of CIP and LVX from wastewater was determined by the generation of high-adsorption metal hydroxides, which aggregate to form suspended flocs.

3.8. Isotherm modelling

3.8.1. Freundlich isotherm

This study utilised the Freundlich adsorption isotherm since it provides suitability for experimental data based on the calculated theoretical data over a broad range of concentrations. The influence of several parameters, including the energies of the active sites and their exponential distribution as well as the surface heterogeneity, were taken into consideration during the experimental modelling. In general, the Freundlich is a reversible process and is not limited to the development of a monolayer. The non-linear model of the Freundlich is expressed as follows [34]:

$$q_e = K_f C_e^{1/n} \tag{9}$$

where K_f and n are Freundlich constants (calculated from the slope) and the intercept of the Freundlich plots, respectively. An n value between 1 and 10 represents a good adsorption potential of the adsorbent. Furthermore, the slope and intercept denote the capacity of adsorption and adsorption intensity, respectively. The correlation coefficient of the plot q_e vs. C_e for CIP and LVX were 0.929 and 0.897, respectively. In addition, the calculated n value from the slope within the range of 1–10 indicates favourable sorption. Therefore, the Freundlich plot suitably fits with the findings. Table 4 lists the K_f and n values.

3.8.2. Langmuir isotherm

The Langmuir isotherm is convenient to represent the deposition of pollutants on the homogenous surface of adsorbents via monolayer adsorption. Eq. (10) describes the Langmuir isotherm model [42]:

$$q_e = \frac{q_m b_l C_e}{1 + b_l C_e} \tag{10}$$

where q_e denotes the adsorption capacity at equilibrium (mg/g), q_m represents the maximum adsorption capacity (mg/g) based on the Langmuir equilibrium constant, b_l is the quantitative convergence between the flocs and pollutants (L/mg), and C_e refers to the concentration of pollutants at equilibrium (mg/L). Besides, R_L is a dimensionless

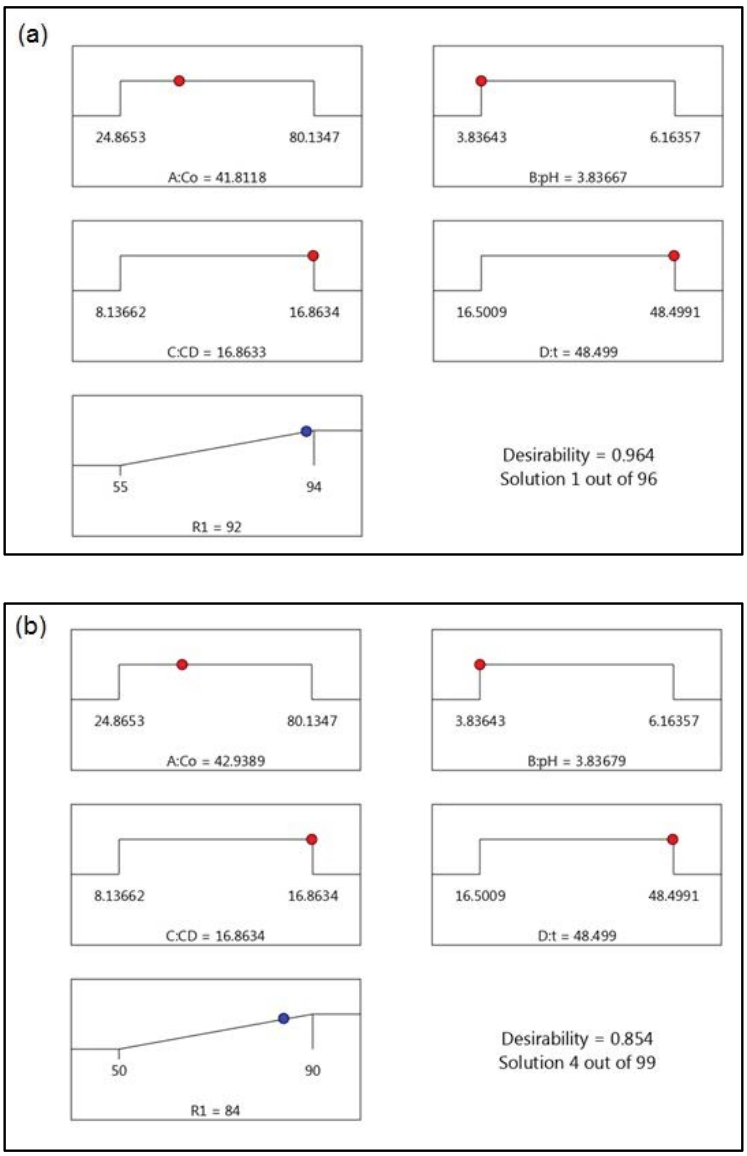

Fig. 3. Maximum efficiency of removing (a) CIP and (b) LVX antibiotics under optimized EC condition.

separation factor that indicates the affinity between the antibiotics and coagulants, as defined in Eq. (11) [33,42]:

$$R_L = \frac{1}{1 + bC_o} \tag{11}$$

where b is the Langmuir isotherm constant (L/mg) and C_o refers to the initial concentration of antibiotics (mg/L). The R_L value of the isotherm can be characterised as follows: linear (R_L = 1), irreversible (R_L = 0), favourable (0 < R_L < 1), and unfavourable (R_L > 1).

Table 4 shows the value of the parameters of the isotherm models with their respective correlation coefficients (R^2). As depicted in Supplementary 5, the Langmuir isotherm model recorded a greater R^2 of 0.958 and 0.927 for CIP and LVX, respectively, compared to those of the Freundlich model, implying a more precise description of the EC process using the Langmuir model. Furthermore, the EC process was categorised as a favourable adsorption process, as indicated by the R_L values between 0 and 1. Overall, the findings of this study suggest the monolayer adsorption of both antibiotics (CIP and LVX) on the adsorbent (flocs of iron hydroxide) surface based on the Langmuirian behaviour, as described by Yoosefian et al. and Mohammed et al.

3.9. Economic evaluation

The operation cost of the EC process was estimated using Eq. (3), where a refers to the price of the electrode material ($2.850 US/kg of 304 stainless steel sheet, IndiaMART), ELC is the quantity of electrode consumed (0.167 kg/m^3), b is the price of the electrical energy ($0.00650 US/kWh) [16], EEC denotes the electrical energy consumed (3.0 kWh/m^3), c represents the price of chemicals used ($0.500 US/kg), and

Table 4
(a) Kinetic model parameters for the removal of CIP and LVX antibiotics under optimized EC condition. (b) The calculated adsorption based on the Langmuir and Freundlich isotherm models for the removal of CIP and LVX under optimized EC condition

(a) Kinetic model	CIP			LVX		
First-order kinetics	C_o	K_1	R^2	C_o	K_1	R^2
	42	0.063	0.828	42	0.053	0.804
Second-order kinetics	C_o	K_2	R^2	C_o	K_2	R^2
	42	0.006	0.986	42	0.004	0.992
Pseudo-first-order kinetics	C_o	K_{app}	R^2	C_o	K_{app}	R^2
	42	0.077	0.965	42	0.065	0.929

(b) Isotherm model	Parameters	CIP	LVX
Freundlich	K_f (mg/g)(L/mg)$^{1/n}$	29	16
	N	1.77	1.42
	R^2	0.929	0.897
Langmuir	q_{max} (mg/g)	142	185
	b (L/mg)	0.24	0.08
	R^2	0.958	0.927
	R_L	0.410	0.673

CC describes the amount of NaCl consumed (0.00050 kg/m^3). Under optimized EC conditions, the operational cost over a single run was estimated at \$0.490 US/m^3. On the other hand, according to Eq. (1), the amount of stainless-steel electrode lost over a single run under optimized EC conditions was 0.167 g (molecular weight of iron = 55.845 g/mol; current = 0.3 A; operation time = 48 min; electron number = 3; Faraday's constant = 96,485 C/mol). Moreover, according to Eq. (2), the amount of EEC over a single run under optimized EC conditions was 3 kWh/m^3 (applied voltage = 12.5 V; operation time = 48 min; current = 0.3 A; sample volume = 1 L).

3.10. Management of EC waste sludges

The EC process is widely known to generate compact waste sludge that does not seep into the environment. The amount of waste sludge generated in the EC process relies on various operating parameters, including the pH value, operation time, concentration of contaminant, and current density [43]. It is highly recommended for future studies to consider the management of sludge in the EC process through numerous methods, such as the removal of sludge contaminants via electrolysis using Ti/RuO_2 plates and sludge de-watering using the microwave technique. Treated sludge can then be used for other applications, such as removing dyes and COD removal [44,45]. Unused treated sludge can also be collected, dried, and disposed of in controlled sanitary landfill sites.

3.11. Comparison of EC with other techniques

The removal efficiencies obtained were compared to previous studies as shown Table 5. Although the removal efficiency of adsorption and advanced oxidation methods is higher than that of electrocoagulation, now the electrocoagulation process is considered a promising process because the equipment of EC is easy and simple for operation. In addition, the problems during the operation of the process can be handled easily. Low operating costs and requiring less maintenance. The sludge created by means of EC process inclines to settle rapidly and easily to be dewatered, mainly consists of metal oxides/hydroxides. Furthermore, sludge production is low. Flocs created by the EC process for similar chemical flocs but, flocs of EC larger, less water contains, it is resistant to acid and more stable, faster separation by filtration. The EC process can be employed in rural areas in which power is not available, as solar panels alone may be enough to achieve accomplish the operation [46–48].

Table 5
Comparison of EC removal efficiency with the other techniques for antibiotic removal from aqueous solutions

Antibiotic	Method	R%	References
Ciprofloxacin	Adsorption	96%	[49]
Levofloxacin	Adsorption	97%	[50]
Ciprofloxacin	Advanced oxidation	98%	[51]
Levofloxacin	Advanced oxidation	100%	[4]
Ciprofloxacin	Electrocoagulation	92%	Current study
Levofloxacin	Electrocoagulation	84%	Current study

4. Conclusion

This study successfully employed the CCD-based RSM to optimize the EC process and achieve effective and cost-effective antibiotics removal from aqueous solutions. The optimization process showed that the pH value, operation time, and current density strongly affected the removal of both antibiotics from aqueous solutions. Although CIP and LVX exhibited similar behaviour since both antibiotics belong to the same FQ family, the removal efficiency of CIP was higher than that of LVX due to the lower solubility of CIP in aqueous solutions. The results showed that the second-order model better suited the experimental results with an R^2 value of 0.986 and 0.992 for CIP and LVX, respectively, and suggested that the adsorption of both antibiotics is controlled by the chemisorption mechanism. In addition, the Langmuir model provided a more precise description of the EC process, while the R_L values between 0 and 1 indicate a favourable adsorption process. Furthermore, the results suggest the single-layer adsorption of antibiotics on the surface of the iron hydroxide flocs, which was regulated via the sweep flocculation mechanism. Overall, the experimental results indicated that the CCD-based RSM significantly improve the operating conditions of the EC process to effectively remove antibiotics. In conclusion, the optimized EC process provided an effective, accurate, and economical technique for antibiotic removal from aqueous solutions.

Acknowledgment

The authors express their appreciation to the University of Baghdad, Baghdad, Iraq, especially the Department of Environmental Engineering and the Department of

Chemical Engineering, and Kerman University of Medical Sciences, Kerman, Iran for supporting the current work.

Funding

This work was supported by the Kerman University of Medical Sciences, Kerman, Iran [grant number 401000766].

References

[1] N.A. Khan, S.U. Khan, S. Ahmed, I.H. Farooqi, M. Yousefi, A.A. Mohammadi, F. Changani, Recent trends in disposal and treatment technologies of emerging-pollutants-a critical review, TrAC, Trends Anal. Chem., 122 (2020) 115744, doi: 10.1016/j.trac.2019.115744.

[2] L. Wang, D. Luo, J. Yang, C. Wang, Metal-organic frameworks-derived catalysts for contaminant degradation in persulfate-based advanced oxidation processes, J. Cleaner Prod., 375 (2022) 134118, doi: 10.1016/j.jclepro.2022.134118.

[3] X. Ma, C. He, Y. Yan, J. Chen, H. Feng, J. Hu, H. Zhu, Y. Xia, Energy-efficient electrochemical degradation of ciprofloxacin by a Ti-foam/PbO_2-GN composite electrode: electrode characteristics, parameter optimization, and reaction mechanism, Chemosphere, 315 (2023) 137739, doi: 10.1016/j.chemosphere.2023.137739.

[4] L. Saya, V. Malik, D. Gautam, G. Gambhir, Balendra, W. Rameshwor Singh, S. Hooda, A comprehensive review on recent advances toward sequestration of levofloxacin antibiotic from wastewater, Sci. Total Environ., 813 (2022) 152529, doi: 10.1016/j.scitotenv.2021.152529.

[5] Z. Kang, X. Jia, Y. Zhang, X. Kang, M. Ge, D. Liu, C. Wang, Z. He, A review on application of biochar in the removal of pharmaceutical pollutants through adsorption and persulfate-based AOPs, Sustainability, 14 (2022) 10128, doi: 10.3390/su141610128.

[6] R. Huang, J. Yang, Y. Cao, D.D. Dionysiou, C. Wang, Peroxymonosulfate catalytic degradation of persistent organic pollutants by engineered catalyst of self-doped iron/carbon nanocomposite derived from waste toner powder, Sep. Purif. Technol., 291 (2022) 120963, doi: 10.1016/j.seppur.2022.120963.

[7] A.S. Oberoi, Y. Jia, H. Zhang, S.K. Khanal, H. Lu, Insights into the fate and removal of antibiotics in engineered biological treatment systems: a critical review, Environ. Sci. Technol., 53 (2019) 7234–7264.

[8] M. Yoosefian, E. Rahmanifar, N. Etminan, Nanocarrier for levodopa Parkinson therapeutic drug; comprehensive benserazide analysis, Artif. Cells Nanomed. Biotechnol., 46 (2018) 434–446.

[9] A. Kausar, K. Naeem, M. Iqbal, Z.-i.-H. Nazli, H.N. Bhatti, A. Ashraf, A. Nazir, H.S. Kusuma, M.I. Khan, Kinetics, equilibrium and thermodynamics of dyes adsorption onto modified chitosan: a review, Z. Phys. Chem., (2021), doi: 10.1515/zpc-2019-1586.

[10] M.S. Thakur, N. Singh, A. Sharma, R. Rana, A.R. Abdul Syukor, M. Naushad, S. Kumar, M. Kumar, L. Singh, Metal coordinated macrocyclic complexes in different chemical transformations, Coord. Chem. Rev., 471 (2022) 214739, doi: 10.1016/j.ccr.2022.214739.

[11] E.-S.I. El-Shafey, H. Al-Lawati, A.S. Al-Sumri, Ciprofloxacin adsorption from aqueous solution onto chemically prepared carbon from date palm leaflets, J. Environ. Sci., 24 (2012) 1579–1586.

[12] H. Raissi, M. Yoosefian, F. Mollania, S. Khoshkhou, Electronic structures, intramolecular interactions, and aromaticity of substituted 1-(2-iminoethylidene) silan amine: a density functional study, Struct. Chem., 24 (2013) 123–137.

[13] M. Chandel, M. Thakur, A. Sharma, D. Pathania, A. Kumar, L. Singh, Chlorophyll sensitized $(BiO)_2CO_3$/$CdWO_4$/rGO nano-hybrid assembly for solar assisted photo-degradation of chlorzoxazone, Chemosphere, 305 (2022) 135472, doi: 10.1016/j.chemosphere.2022.135472.

[14] S. Ahmadzadeh, M. Dolatabadi, Electrochemical treatment of pharmaceutical wastewater through electrosynthesis of iron hydroxides for practical removal of metronidazole, Chemosphere, 212 (2018) 533–539.

[15] K.O. Iwuozor, T.A. Abdullahi, L.A. Ogunfowora, E.C. Emenike, I.P. Oyekunle, F.A. Gbadamosi, J.O. Ighalo, Mitigation of levofloxacin from aqueous media by adsorption: a review, Sustainable Water Resour. Manage., 7 (2021) 100, doi: 10.1007/s40899-021-00579-9.

[16] S.J. Mohammed, M.J. M-Ridha, K.M. Abed, A.A.M. Elgharbawy, Removal of levofloxacin and ciprofloxacin from aqueous solutions and an economic evaluation using the electrocoagulation process, Int. J. Environ. Anal. Chem., (2021) 1–19, doi: 10.1080/03067319.2021.1913733.

[17] M.A. Ibrahim, M.A.A. Shaban, Y.R. Hasan, M.J. M-Ridha, H.A. Hussein, K.M. Abed, S.J. Mohammed, M.H. Muhamad, H.A. Hasan, Simultaneous adsorption of ternary antibiotics (levofloxacin, meropenem, and tetracycline) by sunflower husk coated with copper oxide nanoparticles, J. Ecol. Eng., 23 (2022) 30–42.

[18] M.S. Salman, H.S. Alhares, Q.A. Ali, M.J. M-Ridha, S.J. Mohammed, K.M. Abed, *Cladophora* algae modified with CuO nanoparticles for tetracycline removal from aqueous solutions, Water Air Soil Pollut., 233 (2022) 321, doi: 10.1007/s11270-022-05813-4.

[19] P. Gautam, S. Kumar, Reduction of chemical oxygen demand through electrocoagulation: an exclusive study for hazardous waste landfill leachate, Environ. Sci. Pollut. Res., 29 (2022) 7583–7594.

[20] H. Raissi, A. Khanmohammadi, M. Yoosefian, F. Mollania, Ab initio and DFT studies on 1-(thionitrosomethylene) hydrazine: conformers, energies, and intramolecular hydrogen-bond strength, Struct. Chem., 24 (2013) 1121–1133.

[21] O. Sahu, B. Mazumdar, P. Chaudhari, Treatment of wastewater by electrocoagulation: a review, Environ. Sci. Pollut. Res., 21 (2014) 2397–2413.

[22] U.H. Siddiqua, S. Ali, T. Hussain, M. Iqbal, N. Masood, A. Nazir, Application of multifunctional reactive dyes on the cotton fabric and conditions optimization by response surface methodology, J. Nat. Fibers, 19 (2022) 1094–1106.

[23] S. Barışçı, O. Turkay, Optimization and modelling using the response surface methodology (RSM) for ciprofloxacin removal by electrocoagulation, Water Sci. Technol., 73 (2016) 1673–1679.

[24] R.A. Khera, M. Iqbal, A. Ahmad, S.M. Hassan, A. Nazir, A. Kausar, H.S. Kusuma, J. Niasr, N. Masood, U. Younas, R. Nawaz, M.I. Khan, Kinetics and equilibrium studies of copper, zinc, and nickel ions adsorptive removal on to *Archontophoenix alexandrae*: conditions optimization by RSM, Desal. Water Treat., 201 (2020) 289–300.

[25] J. Jaafari, K. Yaghmaeian, Optimization of heavy metal biosorption onto freshwater algae (*Chlorella coloniales*) using response surface methodology (RSM), Chemosphere, 217 (2019) 447–455.

[26] C.A. Igwegbe, L. Mohmmadi, S. Ahmadi, A. Rahdar, D. Khadkhodaiy, R. Dehghani, S. Rahdar, Modeling of adsorption of methylene blue dye on Ho-$CaWO_4$ nanoparticles using response surface methodology (RSM) and artificial neural network (ANN) techniques, MethodsX, 6 (2019) 1779–1797.

[27] P. Gautam, S. Kumar, Reduction of chemical oxygen demand through electrocoagulation: an exclusive study for hazardous waste landfill leachate, Environ. Sci. Pollut. Res., 29 (2022) 7583–7594.

[28] S. Khandaker, M.F. Chowdhury, M.R. Awual, A. Islam, T. Kuba, Efficient cesium encapsulation from contaminated water by cellulosic biomass based activated wood charcoal, Chemosphere, 262 (2021) 127801, doi: 10.1016/j.chemosphere.2020.127801.

[29] S. Noreen, S. Ismail, S.M. Ibrahim, H.S. Kusuma, A. Nazir, M. Yaseen, M.I. Khan, M. Iqbal, ZnO, CuO and Fe_2O_3 green synthesis for the adsorptive removal of direct golden yellow dye adsorption: kinetics, equilibrium and thermodynamics studies, Z. Phys. Chem., 235 (2021) 1055–1075.

[30] Z. Mohamad, A.A. Razak, S. Krishnan, L. Singh, A. Zularisam, M. Nasrullah, Treatment of palm oil mill effluent using electrocoagulation powered by direct photovoltaic solar system, Chem. Eng. Res. Des., 177 (2022) 578–582.
[31] P. Asaithambi, A.R.A. Aziz, W.M.A.B.W. Daud, Integrated ozone—electrocoagulation process for the removal of pollutant from industrial effluent: optimization through response surface methodology, Chem. Eng. Process. Process Intensif., 105 (2016) 92–102.
[32] D. Ghosh, C. Medhi, M. Purkait, Techno-economic analysis for the electrocoagulation of fluoride-contaminated drinking water, Toxicol. Environ. Chem., 93 (2011) 424–437.
[33] F. Jamali-Behnam, A.A. Najafpoor, M. Davoudi, T. Rohani-Bastami, H. Alidadi, H. Esmaily, M. Dolatabadi, Adsorptive removal of arsenic from aqueous solutions using magnetite nanoparticles and silica-coated magnetite nanoparticles, Environ. Prog. Sustainable Energy, 37 (2018) 951–960.
[34] A. Najafpoor, H. Alidadi, H. Esmaeili, T. Hadilou, M. Dolatabadi, A. Hosseinzadeh, M. Davoudi, Optimization of anionic dye adsorption onto *Melia azedarach* sawdust in aqueous solutions: effect of calcium cations, Asia-Pac. J. Chem. Eng., 11 (2016) 258–270.
[35] S. Ahmadzadeh, A. Asadipour, M. Pournamdari, B. Behnam, H.R. Rahimi, M. Dolatabadi, Removal of ciprofloxacin from hospital wastewater using electrocoagulation technique by aluminum electrode: optimization and modelling through response surface methodology, Process Saf. Environ. Prot., 109 (2017) 538–547.
[36] M. Yoosefian, S. Ahmadzadeh, M. Aghasi, M. Dolatabadi, Optimization of electrocoagulation process for efficient removal of ciprofloxacin antibiotic using iron electrode; kinetic and isotherm studies of adsorption, J. Mol. Liq., 225 (2017) 544–553.
[37] V. Khandegar, A.K. Saroha, Electrocoagulation for the treatment of textile industry effluent–a review, J. Environ. Manage., 128 (2013) 949–963.
[38] I. Epold, M. Trapido, N. Dulova, Degradation of levofloxacin in aqueous solutions by Fenton, ferrous ion-activated persulfate and combined Fenton/persulfate systems, Chem. Eng. J., 279 (2015) 452–462.
[39] B.K. Zaied, M. Rashid, M. Nasrullah, A.W. Zularisam, D. Pant, L. Singh, A comprehensive review on contaminants removal from pharmaceutical wastewater by electrocoagulation process, Sci. Total Environ., 726 (2020) 138095, doi: 10.1016/j.scitotenv.2020.138095.
[40] L. Wang, H. Jiang, H. Wang, P.L. Show, A. Ivanets, D. Luo, C. Wang, MXenes as heterogeneous Fenton-like catalysts for removal of organic pollutants: a review, J. Environ. Chem. Eng., 10 (2022) 108954, doi: 10.1016/j.jece.2022.108954.
[41] M.M. Emamjomeh, M. Sivakumar, Review of pollutants removed by electrocoagulation and electrocoagulation/flotation processes, J. Environ. Manage., 90 (2009) 1663–1679.
[42] H.S. Alhares, M.A.A. Shaban, M.S. Salman, M.J. M-Ridha, S.J. Mohammed, K.M. Abed, M.A. Ibrahim, A.K. Al-Banaa, H.A. Hasan, Sunflower husks coated with copper oxide nanoparticles for Reactive Blue 49 and Reactive Red 195 removals: adsorption mechanisms, thermodynamic, kinetic, and isotherm studies, Water Air Soil Pollut., 234 (2023) 35, doi: 10.1007/s11270-022-06033-6.
[43] S. Safari, M. Azadi Aghdam, H.-R. Kariminia, Electrocoagulation for COD and diesel removal from oily wastewater, Int. J. Environ. Sci. Technol., 13 (2016) 231–242.
[44] H. Gharibi, M.H. Sowlat, A.H. Mahvi, M. Keshavarz, M.H. Safari, S. Lotfi, M.B. Abadi, A. Alijanzadeh, Performance evaluation of a bipolar electrolysis/electrocoagulation (EL/EC) reactor to enhance the sludge dewaterability, Chemosphere, 90 (2013) 1487–1494.
[45] M. Hutnan, M. Drtil, A. Kalina, Anaerobic stabilisation of sludge produced during municipal wastewater treatment by electrocoagulation, J. Hazard. Mater., 131 (2006) 163–169.
[46] M.Y.A. Mollah, R. Schennach, J.R. Parga, D.L. Cocke, Electrocoagulation (EC)—science and applications, J. Hazard. Mater., 84 (2001) 29–41.
[47] K. Chithra, N. Balasubramanian, Modeling electrocoagulation through adsorption kinetics, J. Model. Simul. Syst., 1 (2010) 124–130.
[48] A. Dura, Electrocoagulation for Water Treatment: The Removal of Pollutants Using Aluminium Alloys, Stainless Steels and Iron Anodes, National University of Ireland, Maynooth (Ireland), 2013.
[49] M.J. Ahmed, S.K. Theydan, Fluoroquinolones antibiotics adsorption onto microporous activated carbon from lignocellulosic biomass by microwave pyrolysis, J. Taiwan Inst. Chem. Eng., 45 (2014) 219–226.
[50] T.M. Darweesh, M.J. Ahmed, Batch and fixed bed adsorption of levofloxacin on granular activated carbon from date (*Phoenix dactylifera* L.) stones by KOH chemical activation, Environ. Toxicol. Pharmacol., 50 (2017) 159–166.
[51] H. Alamgholiloo, N.N. Pesyan, R. Mohammadi, S. Rostamnia, M. Shokouhimehr, Synergistic advanced oxidation process for the fast degradation of ciprofloxacin antibiotics using a GO/CuMOF-magnetic ternary nanocomposite, J. Environ. Chem. Eng., 9 (2021) 105486, doi: 10.1016/j.jece.2021.105486.